ACS SENSORS

Article

Cite This: ACS Sens. 2019, 4, 2631−2637

pubs.acs.org/acssensors

A Self-Powered Biosensor with a Flake Electrochromic Display for Electrochemical and Colorimetric Formaldehyde Detection

Xiaoxuan Sun,[†,‡] He Zhang,[†,‡] Shuai Hao,[†,‡] Junfeng Zhai,*[,†] and Shaojun Dong*[,†,‡]

[†]State Key Laboratory of Electroanalytical Chemistry, Changchun Institute of Applied Chemistry, Chinese Academy of Sciences, Changchun 130022, China

[‡]University of Science and Technology of China, Hefei 230026, China

Supporting Information

ABSTRACT: The formaldehyde biosensors with the features of cost effectiveness, high specificity, easy operation, and simplicity are urgently desired in routing and field detection of formaldehyde. Here, we report a new design of an enzymatic self-powered biosensor (ESPB) toward formaldehyde detection. The ESPB involves a formaldehyde dehydrogenase/poly-methylene green/buckypaper bioanode as the sensing electrode and a Prussian blue/Au nanoparticles/carbon fiber paper cathode as the electrochromic display. Formaldehyde acts as the fuel to drive the ESPB, relying on that the concentration of formaldehyde can be determined with the ESPB by both directly measuring the variance in short circuit current and observing the color change of the cathode. By measuring the variance in short circuit current, a linear detection range from 0.01 to 0.35 mM and a calculated detection limit of 0.006 mM are obtained, comparable to or better than those reported before. The color change of the cathode can be distinguished easily and exactly via the naked eye after immersing the ESPB in formaldehyde solution for 90 s with the concentration up to 0.35 mM, covering the permissive level of formaldehyde in some standards associated with environmental quality control. Specially, the formaldehyde concentration can be precisely quantified by analyzing the color change of the cathode digitally using the equation of $B/(R + G + B)$. In the following test of real spiked samples of tap water and lake water, the recovery ratios of formaldehyde with the concentrations from 0.010 to 0.045 mM are tested to be between 95 and 100% by both measuring the variance in short circuit current and analyzing the color change of the cathode digitally. In addition, the ESPB exhibits negligible interference from acetaldehyde and ethanol and can be stored at 4 °C for 21 days with a loss of less than 8% in its initial value of short circuit current. Therefore, the ESPB with the capability of working like disposable test paper can be expected as a sensitive, simple, rapid, cost-effective colorimetric method with high selectivity in routing and field formaldehyde detection.

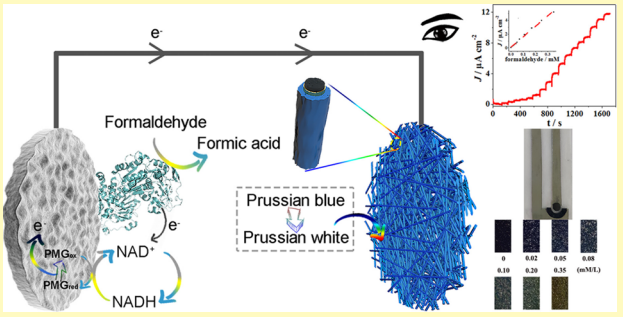

KEYWORDS: *self-powered biosensor, formaldehyde dehydrogenase, flake electrochromic cathode, disposable, visual detection*

Because of its well-known serious harmfulness to human beings, the detection of formaldehyde at low concentration is very important from the environmental and medical viewpoints.[1] Standard methods for formaldehyde detection, such as spectrophotometry,[2−4] spectrofluorometric,[5,6] and chromatographic[7,8] methods, have proven the ability to detect formaldehyde at sub-ppm or ppb levels, but they suffer from high-cost equipment, complicated operation procedure, and especially the requirement of an external power source.[9] To overcome these problems, many efforts have been devoted to design formaldehyde biosensors.[10] For example, Korpan and co-workers reported a potentiometric biosensor with a linear formaldehyde detection range from 2 to 200 mM, by combining an immobilized enzyme and pH-sensitive field-effect transistor.[11] Shimomura et al. presented an amperometric formaldehyde biosensor with a detection limit of 1.2 μM and a long storage period of over 80 days.[12] Although significant progress has been made, the improvement in terms of simplicity, cost efficiency, sensitivity, and so on is still desired urgently for routing and field formaldehyde detection.

There is growing interest in enzymatic self-powered biosensors (ESPBs), which can be due to their capability in powering signaling devices and the obvious advantages of high selectivity and high sensitivity.[13,14] ESPB is commonly composed of two electrodes to yield a galvanic cell, and at least one of them is an enzyme-modified electrode used as the sensing electrode. The variances in performance including open circuit potential, short cut current, and maximum power density are referred to the concentration of the analyte. Although various enzymatic self-powered electrochemical biosensors have been designed to detect, for example, glucose,[15] lactate,[16] cholesterol,[17] cyanide,[18] and mercury,[19]

Received: May 17, 2019
Accepted: August 23, 2019
Published: August 23, 2019

DOI: 10.1021/acssensors.9b00917
ACS Sens. 2019, 4, 2631−2637

to the best of our knowledge, ESPB toward formaldehyde detection has not yet been reported.

An amazing trend in the development of ESPB is making the detection results visible.[20] Two main approaches have been proposed in designing such biosensors, and based on which, several impressive designs have been reported. One approach is to power light or mechanical components by using a well-designed electric board. For example, Sode and his co-workers reported the use of a capacitor as a transducer to power a stepper motor in an enzymatic self-powered glucose biosensor where the concentration of glucose was referred to the torque and rotational speed of the stepper motor.[21] The other approach is the use of an electrochromic display such as a Prussian blue (PB) display to construct a galvanic cell with enzymatic electrodes, and the qualitative and even quantitative information of the concentration of analyte can be obtained easily by observing the color change of the electrochromic display directly via the naked eye or digital camera.[22,23] It should be pointed that, compared to the use of "silicon-based electronics", the use of the electrochromic display is more favorable in designing low-cost, portable, and disposable ESPB, as it can dramatically simplify biosensors.

This work demonstrates a design of colorimetric ESPB toward formaldehyde detection, as shown in Figure 1. The

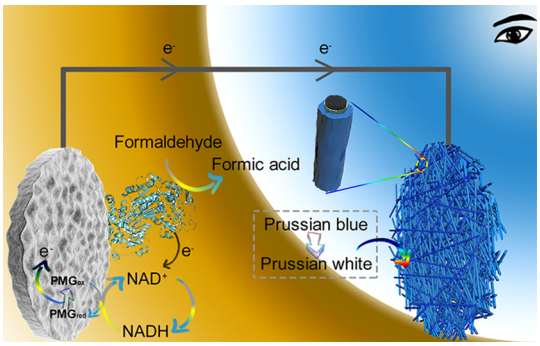

Figure 1. Working principle of the ESPB.

ESPB is composed of a formaldehyde dehydrogenase (FDH)/poly-methylene green (PMG)/buckypaper (BP) bioanode as the sensing electrode and a Prussian blue (PB)/Au nanoparticles (Au NPs)/carbon fiber paper (CFP) cathode as the electrochromic display wherein formaldehyde as the fuel of ESPB is catalytically oxidized at the bioanode and electrons are transferred to the cathode through an external circuit, thereby leading to the color change of the cathode, namely, PB reduction. Therefore, the successful detection of formaldehyde with the ESPB can be achieved by both measuring the variance in short circuit current and observing the color change of the cathode. When measuring the variance in short circuit current, the ESPB exhibits a linear formaldehyde detection range of 0.01 to 0.35 mM with a calculated detection limit of as low as 0.006 mM (S/N = 3). Importantly, in the case of colorimetric detection, the cathode of ESPB changes its color from initial dark blue to eventually dark yellow when varying the concentration of formaldehyde from 0.00 to 0.35 mM, covering the permissive level of formaldehyde in some standards associated with environmental quality control. The quantitative detection has also been achieved by analyzing the RGB values of the cathode images captured by a smartphone. The ESPB can thus be expected to work like disposable test paper in routing and field detection of formaldehyde, with the advantages of such as cost effectiveness, easy operation, and no requirement of external power supply and even signaling devices.

EXPERIMENTAL SECTION

Reagents and Chemicals. Chloroauric acid, potassium ferricyanide, ferric chloride, potassium chloride, formaldehyde solution, hydrochloric acid, potassium dihydrogen phosphate, and dipotassium hydrogen phosphate were purchased from Beijing Chemical Reagent Company (A. R. analytical reagent grade). Paraffin was purchased from Sinopharm Chemical Reagent Co. Ltd., China. Formaldehyde dehydrogenase (FDH, E.C.1.2.1.46, 4.8 U mg^{-1}) and methylene green (MG, 80%) were purchased from Yuanye Biotechnology Co., Ltd., Shanghai, China. 1-Pyrenebutyric acid (PBA) (97%) was purchased from Sigma-Aldrich. Primary buckypaper (BP) was purchased from NanoTechLabs, Inc. (Yadkinville, NC). Single-sided indium tin oxide (ITO) conducting glass (30−60 cm^{-2}) was purchased from Huananxiangcheng, Shenzhen, China. Single-sided ITO-coated polyethylene terephthalate (ITO-PET, 15 ± 2 Ω cm^{-2}, light transmittance >76%) was bought from Kaivo Optoelectronic Technology Co. Ltd., China. Nicotinamide adenine dinucleotide (NAD^+) and the reduced form nicotinamide adenine dinucleotide (NADH) were purchased from Gen-view Scientific Inc. A phosphate buffer solution (0.1 M, pH 6.0, PBS) was employed as the supporting electrolyte. The FDH stock solution (1 mg mL^{-1}) was prepared by dissolving the enzyme powder in 0.01 M phosphate buffer solution (PBS) at pH 7.0 and kept at −20 °C immediately. All other chemicals were of analytical grade, and all aqueous solutions were prepared with ultrapure water (>18.25 MΩ cm) obtained with a water purifier purchased from Hitech Instruments Co., Ltd., Shanghai, China.

Electrochemical experiments were performed with a CHI832B electrochemical workstation. In the case of a standard three-electrode test, a KCl-saturated Ag/AgCl electrode and a Pt coil were used as reference and counter electrodes, respectively. All potentials given here were versus the Ag/AgCl electrode. Scanning electron microscopy (SEM) images were obtained with an XL30ESEM FEG SEM (Philips, Netherlands) at an accelerating voltage of 20 kV, equipped with an energy-dispersive spectrometer (EDS). X-ray diffraction (XRD) analysis was carried out on a D8 Advance (Bruker, Germany) diffractometer with Cu Kα radiation (λ = 1.5406 Å).

Preparation of FDH/PMG/BP Bioanode. The primary BP with a diameter of 3 mm was first immersed in 2 mg mL^{-1} PBA DMF solution under mild and slow stirring for 1 h, then rinsed with ultrapure water, and dried at 60 °C in an oven.[24] The adsorption of PBA could enhance the hydrophilicity of the primary BP (Figure S2) and thus facilitate the following electrochemical polymerization of PMG. Unless stated otherwise, all the BP used in the electrochemical experiments and the fabrication of bioanode was treated with PBA. Subsequently, PMG was electropolymerized on the BP surface by cycling the potential at a scan rate of 50 mV s^{-1} between −0.5 and 1.3 V for two cycles in a fresh MG solution.[25,26] The MG solution was prepared by dissolving 0.5 mM MG and 0.1 M $NaNO_3$ in 0.01 M nitrogen-saturated borate buffer (pH 9.1). After polymerization, the PMG-modified BP (PMG/BP) was rinsed with ultrapure water and air-dried. For FDH confinement, a droplet of 10 μL of FDH solution was cast on the PMG/BP substrate. By evaporating the solution at 4 °C overnight, the FDH/PMG/BP bioanode was obtained.

Preparation of PB/Au NPs/CFP Cathode. A piece of CFP was washed by sequential sonication in ethanol and water for a few minutes. Then Au NPs were electrochemically deposited on the CFP surfaces via potential cycling at a scan rate of 5 mV s^{-1} for one cycle between −0.9 and 0.6 V in a 10 mM $HAuCl_4$ solution.[27] The prepared Au NPs/CFP electrode was rinsed with ultrapure water and air-dried. PB was deposited spontaneously on Au NPs/CFP surfaces to yield the PB/Au NPs/CFP cathode by immersing the Au NPs/CFP in a freshly prepared solution containing 0.1 M KCl, 0.1 M HCl, 10 mM $K_3[Fe(CN)_6]$, and 10 mM $FeCl_3$ for 5 min. In order to investigate the influence of the PB amount on the performance of the

DOI: 10.1021/acssensors.9b00917
ACS Sens. 2019, 4, 2631−2637

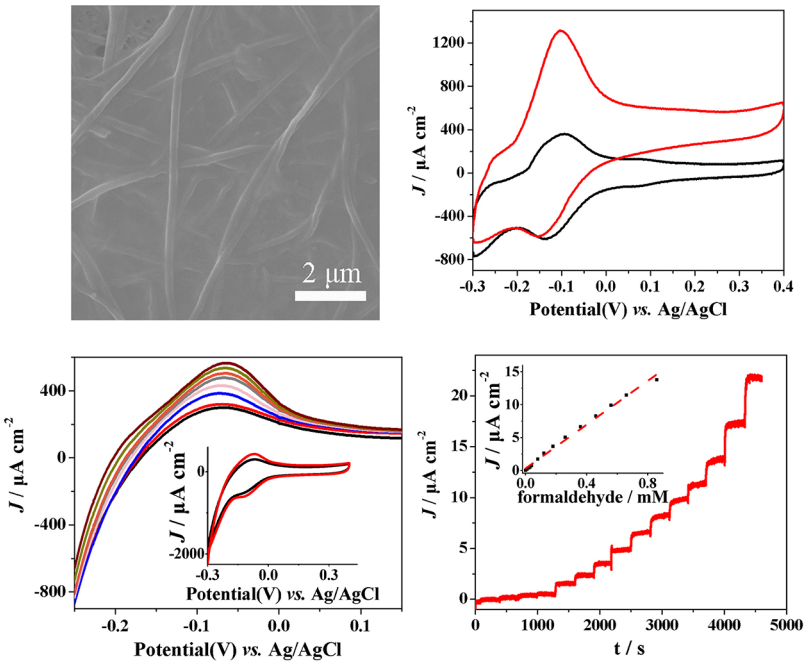

Figure 2. (A) SEM image of the PMG/BP electrode. (B) Cyclic voltammograms of the PMG/BP electrode in 0.1 M PBS, pH 6.0, with (red) and without (black) 5 mM NADH at a scan rate of 5 mV s^{-1}. (C) Linear sweep voltammograms of the FDH/PMG/BP electrode with different formaldehyde concentrations (0, 2, 4, 6, 8, 10, 12, and 14 mM; arranged from bottom to top, respectively) (inset: cyclic voltammograms in the absence and presence of 4 mM formaldehyde) at a scan rate of 5 mV s^{-1}. (D) Chronoamperometric response of the FDH/PMG/BP electrode with successive additions of formaldehyde recorded at 0 V (inset: calibration curve of formaldehyde concentration versus anodic current).

ESPB, immersion times of 3, 4, and 6 min were also used to prepare the cathodes loading different amounts of PB.[28] The prepared PB/Au NPs/CFP cathodes were then thoroughly rinsed with ultrapure water to remove the physically adsorbed species.

Preparation of the Disposable ESPB. In a typical preparation procedure, two ITO-PET as soft current collectors were first stuck on filter paper with double-sided adhesive tape, the sizes and shapes of which are shown in Figure S1. The filter paper was then immersed in melting paraffin wax to construct a hydrophobic barrier.[29] After being cooled down to room temperature, the paraffin on ITO-PET surfaces was removed by peeling off the protecting film of ITO-PET. The FDH/PMG/BP bioanode and PB/Au NPs/CFP cathode were confined on ITO-PET collectors by silver paint, as shown in Figure S8. The two separate ITO-PET collectors were connected with silver conductive tape to form an external circuit when sensing formaldehyde in the colorimetric method. NAD^+ and NADH were dispersed in PBS as charge transfer in the enzymatic reaction.[30]

RESULTS AND DISCUSSION

Characterization of FDH/PMG/BP Bioanode. BP with good biocompatibility, high electrical conductivity, and large specific surface area is chosen as the support to construct the bioanode in this work.[31] PMG has been well studied as a two-electron mediator to shuttle electrons from NADH to electrodes where the oxidized PMG can oxidize NADH, subsequently regenerating the reduced PMG and the bioactive NAD^+.[32,33] Therefore, PMG is adopted as the appropriate mediator to overcome the drawbacks from the slow heterogeneous kinetics and high overpotential of NADH oxidation.[25] As shown in Figure S3, the BP used here has large amounts of interconnected macropores, which can facilitate the mass transport for the following electrochemical polymerization.[34] After exposing the BP to MG monomer under potential cycling between −0.50 and 1.30 V, almost all of the macropores of BP are filled with a precipitate, indicating the successful deposition of PMG on BP surfaces.

Figure 2B and as a comparison Figure S4 show the cyclic voltammograms (CVs) obtained with a PMG/BP electrode and a BP electrode in a 0.1 M PBS (pH 6.0), respectively. No redox behavior can be observed for the BP electrode in the potential range of −0.20 and 0 V, while, in the case of the PMG/BP electrode, there is a pair of well-defined redox peaks located at −0.10 and −0.14 V, which can be attributed to the characteristic redox behavior of PMG,[35,36] further demonstrating the successful deposition of PMG. After adding 5 mM NADH, the onset potential of the anodic reaction negatively shifts from −0.15 to −0.20 V, and the anodic peak current increases from 380 to over 1300 μA cm^{-2} at the PMG/BP electrode. The negatively shifted onset potential and the dramatically increased peak current strongly demonstrate the ability of PMG to catalyze the electrochemical oxidation of NADH. Moreover, it is noticeable that the electrochemical oxidation of NADH at the BP electrode starts at −0.10 V and the anodic peak current at approximately 0.10 V is less than 250 μA cm^{-2}. This result suggests a slow kinetics and a large overpotential of NADH oxidation at the BP electrode and of course indicates the importance of PMG in boosting the output of the bioanode, which, in turn, ensures that the color change of the cathode can be initiated with a small bioanode.

FDH is deposited on the PMG/BP electrode by drop casting to yield the FDH/PMG/BP bioanode. Figure 2C shows the linear sweep voltammograms (LSVs) of formaldehyde with different concentrations at the FDH/PMG/BP bioanode. It can be observed that the anodic current increases gradually with the increment of the concentration of formaldehyde. The increase in anodic current can be attributed to the generation of NADH as an enzymatic reaction product being oxidized by PMG. The formaldehyde-concentration-dependent anodic current also confirms that the FDH/PMG/BP electrode can be used as a sensing electrode for formaldehyde detection. In

DOI: 10.1021/acssensors.9b00917
ACS Sens. 2019, 4, 2631−2637

addition, although the anodic peak position shows a slight positive shift with the increment in the concentration of formaldehyde, it is still located at a potential of less than −0.05 V for 14 mM formaldehyde, much lower than the redox potential of PB/PW. This fact indicates the feasibility of the PB-based solid cathode in constructing a self-powered biofuel cell with the FDH/PMG/BP bioanode.[37]

Figure 2D exhibits the amperometric response of the FDH/PMG/BP electrode to successive additions of formaldehyde recorded at 0 V where the bioanodic current increases immediately after the addition of formaldehyde and approaches a steady state within 10 s. The calibration curve, shown as the inset of Figure 2D, reveals a linear formaldehyde detection range of 0.01 to 0.85 mM, demonstrating the excellent promise of the FDH/PMG/BP electrode in formaldehyde detection.

Characterization of PB/Au NPs/CFP Cathode. The PB/Au NPs/CFP cathode is prepared via a two-step method including the electrochemical deposition and the chemical deposition (Figure 3A). Au NPs were first deposited on CFP

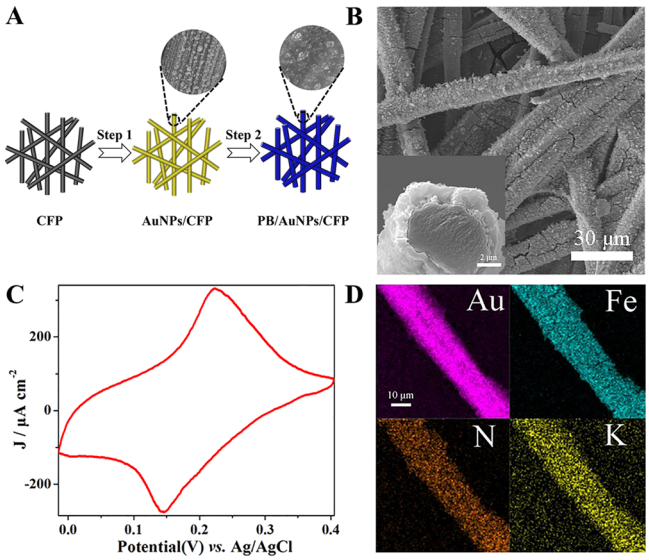

Figure 3. (A) Schematic illustration of the preparation procedure of PB/Au NPs/CFP cathode. (B) SEM images of the PB/Au NPs/CFP cathode. (C) Cyclic voltammograms of the PB/Au NPs/CFP cathode in 0.1 M PBS, pH 6.0, at a scan rate of 5 mV s^{-1}. (D) Elemental mapping images of the PB/Au NPs/CFP electrode.

electrochemically according to the previous work with a slight modification.[27] The CFP is composed of carbon fiber with smooth and clean surfaces,[38] and after the electrochemical deposition, a large number of particles with sizes from 100 to 200 nm can be observed at the surfaces of carbon fibers (Figure S5). The XRD pattern of these particles deposited can be indexed to a face-centered cubic structure of metal gold (JCPDS No. 04-0784), and the diffraction peaks at 38.2, 44.4, 64.6, and 77.5° can be assigned to the (111), (200), (220), and (311) reflections, respectively (Figure S6).[39] The results from SEM and XRD characterization strongly demonstrate the successful deposition of Au NPs. The use of electrochemical deposition is because it is a simple, rapid, convenient, and controllable method and, most importantly, it can endow the Au NPs with a "clean" surface for the following chemical deposition of PB.[40,41]

PB is then deposited on Au NPs/CFP chemically by immersing the latter in a solution containing $K_3[Fe(CN)_6]$ and $FeCl_3$ for a period of time.[40] For example, after immersion for 5 min, the characteristic redox peaks of PB located at 0.23 and 0.14 V for anodic and cathodic reactions, respectively, can be obtained at the Au NPs/CFP electrode (Figure 3C), directly indicating the successful deposition of PB.[40] The PB deposited on carbon fibers forms a film with thickness varying from 1 to 2 μm, as shown in Figure 3B. No obvious diffraction peak for PB can be observed in the XRD measurement, suggesting an amorphous phase of PB deposited. Although the reaction between Au NPs and ferricyanide can induce the dissolution of Au NPs,[42] the XRD pattern of Au NPs can still be observed after immersion, demonstrating the survival of Au NPs from dissolution. The element mapping images of the PB/Au NPs/CFP cathode reveal the existence and overlap of Au, Fe, N, and K, further confirming the successful deposition of Au NPs and PB films on carbon fiber surfaces and therefore the fabrication of the PB/Au NPs/CFP cathode (Figure 3D).

Characterization and Performance of Self-Powered Biosensor. A membrane-less ESPB toward formaldehyde detection is constructed by coupling the FDH/PMG/BP bioanode and the PB/Au NPs/CFP cathode. The PB/Au NPs/CFP cathode used is prepared by immersing the Au NPs/CFP in a solution of $K_3[Fe(CN)_6]$ and $FeCl_3$ for 5 min. An open circuit potential of 0.44 V and a maximum power density of 25.5 μW cm^{-2} are obtained in the presence of 9 mM formaldehyde (Figure 4A), demonstrating the nature of formaldehyde as fuel to drive the ESPB. The feasibility of the ESPB in formaldehyde detection was evaluated by measuring the short circuit current under successive addition of formaldehyde, as shown in Figure 4B. Obviously, the short circuit current of the ESPB increases with the addition of formaldehyde and reaches 90% of the maximum value within 10 s. The calibration curve shown as the inset of Figure 4B reveals a linear response to formaldehyde in the concentration range from 0.01 to 0.35 mM (R^2 = 0.99), narrower than that obtained at the FDH/PMG/BP bioanode operated in amperometric mode as mentioned above, due to the limit from the PB/Au NPs/CFP cathode. The detection limit is estimated to be 0.006 mM from the calibration curve (S/N = 3), comparable to or better than those reported for enzymatic and non-enzymatic biosensors.[43,44] The selectivity of ESPB against the possible interfering species has been investigated. As shown in Figure 4C, no obvious change in the short circuit current of ESPB can be observed after the addition of acetaldehyde and ethanol, while a sharp increment of short circuit current appears immediately after the addition of formaldehyde, indicating the negligible interference from acetaldehyde and ethanol to formaldehyde detection.

The storage stability of the ESPB at 4 °C has been determined by measuring the decrease of the short circuit current corresponding to 0.2 mM formaldehyde during storage. Figure 4D shows a plot of short circuit current versus storage time wherein it can be seen that the short circuit current remains over 92% of its initial value after 21 days of storage and over 80% after 31 days of storage.

The feasibility of the ESPB working like disposable test paper in the colorimetric detection of formaldehyde is further investigated by immersing the ESPB in solutions spiked with formaldehyde of different concentrations.

The immersion time (or contact time) is optimized to be 90 s because the short circuit currents of the ESPB decrease

DOI: 10.1021/acssensors.9b00917
ACS Sens. 2019, 4, 2631−2637

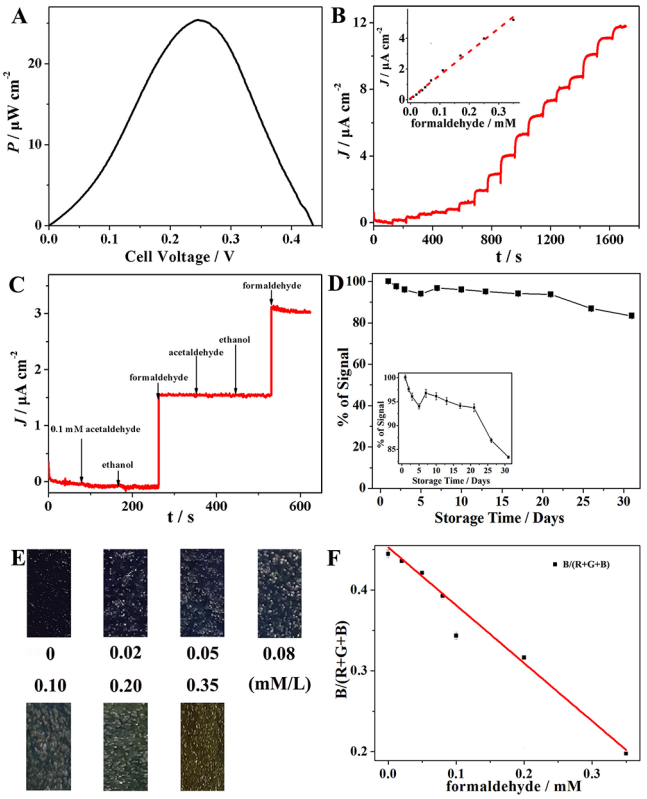

Figure 4. (A) Power output of the ESPB in 0.1 M PBS, pH 6.0, at 9 mM formaldehyde. (B) Short circuit current of the ESPB with successive additions of formaldehyde (inset: calibration curve of short circuit current versus formaldehyde concentrations). (C) Short circuit current to successive addition of 0.1 mM acetaldehyde, 0.1 mM ethanol, and 0.1 mM formaldehyde (D) Variance in short circuit current to 0.2 mM formaldehyde with the storage time (normalized to the initial value). (E) Colorimetric card composed of the color of cathode captured after immersion in formaldehyde solutions with different concentrations for 90 s. (F) Plot of formaldehyde concentrations versus the value of $B/(R + G + B)$.

rapidly at first and then reach a steady state after about 90 s, and further prolonging the immersion time (or contact time) cannot significantly increase the charge flowing in the circuit when sensing low-concentrated formaldehyde (0.01 mM), as shown in Figure S7. As shown in Figure 4E, the color of the PB/Au NPs/CFP cathode gradually changed from the initial dark blue to slight blue, then to slight green, and eventually to dark yellow, when varying the concentration of formaldehyde from 0 to 0.35 mM. It should be noticed that the function of Au NPs in the design of the cathode is serving not only as the catalyst or reactant for PB formation but also as a bright dye with a yellow color to change the background color from black to dark yellow, thus enabling the color change of the cathode to be distinguished via the naked eye more easily and exactly.

The detection range of formaldehyde via the naked eye is from 0.00 to 0.35 mM (Figure 4E), covering the permissive level of formaldehyde in some standards associated with environmental quality control. For example, the permissive level of formaldehyde in drinking source water is 0.03 mM in China (GB3838-2002), and World Health Organization recommends a value of 0.08 ppm among indoor air (corresponding to 0.25 mM in aqueous solution at room temperature according the work of Dong and Dasgupta)[45] as the permissible limit of short-term exposure to formaldehyde. Furthermore, as shown in Figure 4F, the captured images (Figure 4E) by a smartphone are further digitized into an RGB value matrix with the aid of MATLAB software, and a good linear relationship (R^2 = 0.98) between the concentration of formaldehyde and the value of $B/(R + G + B)$ can be obtained, indicating that the quantitative detection of formaldehyde can be fulfilled by integrating the ESPB with a smartphone in the future.

The influence of the PB amount on colorimetric detection of formaldehyde has also been investigated, as shown in Figure S9. It can be observed that the lower amount of PB can lead to a more significant color change of the cathode during testing especially in the presence of high-concentrated formaldehyde due to the fact that the lower amount of PB results in the higher ratio of PB reduced when the same charge flows in the circuit. Moreover, the higher amount of PB results in the darker background color (initial color) of the cathode in Figure S9. A good linear relationship between the concentration of formaldehyde and the value of $B/(R + G + B)$ has been achieved with the cathode loading different PB amounts. The largest slope (highest sensitivity) is obtained with the cathode prepared by immersing the Au NPs/CFP in a solution of $K_3[Fe(CN)_6]$ and $FeCl_3$ for 5 min, indicating that both the background color and the ratio of PB reduced can affect the sensitivity of ESPB in the colorimetric detection of formaldehyde by using the value of $B/(R + G + B)$. Therefore, the amount of PB plays an important role in improving the sensitivity of ESPB by adjusting the background color and the ratio of PB reduced. The cathode prepared by immersing the Au NPs/CFP in a solution of $K_3[Fe(CN)_6]$ and $FeCl_3$ for 5 min is chosen as the optimal cathode in the detection of the spiked real samples.

Application to the Spiked Real Samples. In order to demonstrate the feasibility of the ESPB in practical applications, the detection of formaldehyde was performed in

Table 1. Determination of Formaldehyde Content in Real Water Samples

water samples	added formaldehyde (mM L^{-1})	measured (mM L^{-1})	recovery (%)	RSD (%, n = 3)	method
tap water	0.010	0.0098	98.0	3.3	short circuit current (SCC)
	0.020	0.020	100	2.7	SCC
	0.045	0.044	97.8	2.3	SCC
Chagan Lake water	0.010	0.0096	96.0	6.3	SCC
	0.020	0.020	100	5.3	SCC
	0.045	0.044	97.8	5.7	SCC
	0.010	0.0097	97.0	6.8	$B/(R + G + B)$
	0.030	0.029	96.7	5.2	$B/(R + G + B)$
	0.045	0.045	100	2.8	$B/(R + G + B)$

DOI: 10.1021/acssensors.9b00917
ACS Sens. 2019, 4, 2631−2637

spiked real samples of tap and lake water from our institute and Chagan Lake of Jilin Province, China, respectively, with the concentrations near the permissive level (0.03 mM) in drinking water sources of China. As shown in Table 1, the recovery ratios of formaldehyde with concentrations from 0.010 to 0.045 mM in both water samples are between 95 and 100% in the case of measuring the short circuit current, showing that ESPB is capable of determining formaldehyde in a real sample matrix.

In particular, excellent recovery ratios (95−100%) of formaldehyde from 0.010 to 0.045 mM in Chagan Lake water samples have also been obtained by analyzing RGB values. Therefore, the ESPB can be expected as a portable and disposable biosensor like test paper for routing and field formaldehyde detection without the requirement of external power supply.

CONCLUSIONS

In summary, the ESPB toward formaldehyde detection has been constructed successfully by coupling the FDH/PMG/BP bioanode and PB/Au NPs/CFP cathode. Formaldehyde is the fuel of the ESPB, and an open circuit potential of 0.44 V and a maximum power density of 25.5 μW cm^{-2} have been obtained at 9 mM formaldehyde. By measuring the variance in the short circuit current, a linear formaldehyde detection range of 0.01 to 0.35 mM and a detection limit of as low as 0.006 mM have been obtained, which are comparable to or better than those reported for other enzymatic or non-enzymatic sensors previously. The ESPB shows high selectivity to formaldehyde, as there is no interference from acetaldehyde and ethanol. The short circuit currents of ESPB to 0.2 mM formaldehyde remain over 92 and 80% of its initial value after 21 days and 31 days of storage in air at 4 °C, suggesting good long-term storage stability. Importantly, the color change of the cathode can be distinguished easily and exactly via the naked eye with the concentration up to 0.35 mM, and quantitative detection can be achieved by analyzing the color change using the equation of $B/(R + G + B)$. In a spiked real sample test, the recovery ratios of formaldehyde with concentrations from 0.010 to 0.045 mM are determined to be between 95 and 100% by both measuring the short circuit current and analyzing the color change digitally, demonstrating the feasibility of the ESPB in practical applications. It is worth mentioning that the detection range of the ESPB covers well for example the permissive level in drinking water sources in China and the permissive short-term exposure limit recommended by WHO. Therefore, as a cost-effective, time-saving, convenient, disposable, and portable biosensor with the capability of working like test paper, the ESPB shows good promise in routine and field formaldehyde detection.

ASSOCIATED CONTENT

Supporting Information

The Supporting Information is available free of charge on the ACS Publications website at DOI: 10.1021/acssensors.9b00917.

Size and shape of the ITO-PET (Figure S1); images of the contact angles of a drop of water on primary BP and BP surfaces (Figure S2); SEM image of a BP electrode (Figure S3); CVs obtained at a BP electrode with (red) and without (black) NADH (Figure S4); SEM image of the Au NPs/CFP electrode (Figure S5); XRD patterns of CFP, Au NPs/CFP, and PB/Au NPs/CFP electrodes (Figure S6); chronoamperometric responses of ESPB to formaldehyde (Figure S7); photograph of the ESPB (Figure S8); colorimetric cards and calibration curves obtained with the ESPB composed of the cathodes loading different amounts of PB; comparison of optical sensitivity of ESPB with cathode of different PB amounts (Figure S9) (PDF)

AUTHOR INFORMATION

Corresponding Authors

*E-mail: jfzhai@ciac.ac.cn (J.Z.).
*E-mail: dongsj@ciac.ac.cn (S.D.).

ORCID

Shaojun Dong: 0000-0003-3197-7204

Notes

The authors declare no competing financial interest.

ACKNOWLEDGMENTS

This work was supported by the National Natural Science Foundation of China (Grant No. 21675151) and MOST, China (Grant No. 2016YFA0203203).

REFERENCES

(1) Duong, A.; Steinmaus, C.; McHale, C. M.; Vaughan, C. P.; Zhang, L. Reproductive and developmental toxicity of formaldehyde: A systematic review. *Mutat. Res., Rev. Mutat. Res.* **2011**, *728*, 118−138.

(2) Cui, X.; Fang, G.; Jiang, L.; Wang, S. Kinetic spectrophotometric method for rapid determination of trace formaldehyde in foods. *Anal. Chim. Acta* **2007**, *590*, 253−259.

(3) Khanmohammadi, M.; Garmarudi, A. B.; Elmizadeh, H.; Roochi, M. B. Spectrophotometric evaluation of the photocatalytic degradation of formaldehyde by Fe_2O_3-TiO_2 nano hybrid. *J. Ind. Eng. Chem.* **2014**, *20*, 1841−1844.

(4) Yasri, N. G.; Seddik, H.; Mosallb, M. A. Spectrophotometric determination of formaldehyde based on the telomerization reaction of tryptamine. *Arab. J. Chem.* **2015**, *8*, 487−494.

(5) Motyka, K.; Mikuška, P. Continuous fluorescence determination of formaldehyde in air. *Anal. Chim. Acta* **2004**, *518*, 51−57.

(6) Zhao, X. Q.; Zhang, Z. Q. Microwave-assisted on-line derivatization for sensitive flow injection fluorometric determination of formaldehyde in some foods. *Talanta* **2009**, *80*, 242−245.

(7) Bianchi, F.; Careri, M.; Musci, M.; Mangia, A. Fish and food safety: Determination of formaldehyde in 12 fish species by SPME extraction and GC-MS analysis. *Food Chem.* **2007**, *100*, 1049−1053.

(8) Gu, Z. Y.; Wang, G.; Yan, X. P. MOF-5 metal-organic framework as Sorbent for in-field sampling and preconcentration in combination with thermal desorption GC/MS for determination of atmospheric formaldehyde. *Anal. Chem.* **2010**, *82*, 1365−1370.

(9) Ling, Y. P.; Heng, L. Y. A potentiometric formaldehyde biosensor based on immobilization of alcohol oxidase on acryloxysuccinimide-modified acrylic microspheres. *Sensors* **2010**, *10*, 9963−9981.

(10) Noor Aini, B.; Siddiquee, S.; Ampon, K. Development of formaldehyde biosensor for determination of formalin in fish samples; malabar red snapper (lutjanus malabaricus) and longtail tuna (thunnus tonggol). *Biosensors* **2016**, *6*, 32.

(11) Korpan, Y. I.; Gonchar, M. V.; Sibirny, A. A.; Martelet, C.; El'skaya, A. V.; Gibson, T. D.; Soldatkin, A. P. Development of highly selective and stable potentiometric sensors for formaldehyde determination. *Biosens. Bioelectron.* **2000**, *15*, 77−83.

(12) Shimomura, T.; Itoh, T.; Sumiya, T.; Mizukami, F.; Ono, M. Electrochemical biosensor for the detection of formaldehyde based on enzyme immobilization in mesoporous silica materials. *Sens. Actuators, B* **2008**, *135*, 268−275.

DOI: 10.1021/acssensors.9b00917
ACS Sens. 2019, 4, 2631−2637

(13) Grattieri, M.; Minteer, S. D. Self-powered biosensors. *ACS sensors* **2018**, *3*, 44−53.
(14) Katz, E.; Bückmann, A. F.; Willner, I. Self-powered enzyme-based biosensors. *J. Am. Chem. Soc.* **2001**, *123*, 10752−10753.
(15) Slaughter, G.; Kulkarni, T. A self-powered glucose biosensing system. *Biosens. Bioelectron.* **2016**, *78*, 45−50.
(16) Hickey, D. P.; Reid, R. C.; Milton, R. D.; Minteer, S. D. A self-powered amperometric lactate biosensor based on lactate oxidase immobilized in dimethylferrocene-modified LPEI. *Biosens. Bioelectron.* **2016**, *77*, 26−31.
(17) Sekretaryova, A. N.; Beni, V.; Eriksson, M.; Karyakin, A. A.; Turner, A. P. F.; Vagin, M. Y. Cholesterol self-powered biosensor. *Anal. Chem.* **2014**, *86*, 9540−9547.
(18) Deng, L.; Chen, C.; Zhou, M.; Guo, S.; Wang, E.; Dong, S. Integrated self-powered microchip biosensor for endogenous biological cyanide. *Anal. Chem.* **2010**, *82*, 4283−4287.
(19) Wen, D.; Deng, L.; Guo, S.; Dong, S. Self-powered sensor for trace hg^{2+} detection. *Anal. Chem.* **2011**, *83*, 3968−3972.
(20) Slaughter, G.; Kulkarni, T. Highly selective and sensitive self-powered glucose sensor based on capacitor circuit. *Sci. Rep.* **2017**, *7*, 1471.
(21) Hanashi, T.; Yamazaki, T.; Tanaka, H.; Ikebukuro, K.; Tsugawa, W.; Sode, K. The development of an autonomous self-powered bio-sensing actuator. *Sens. Actuators, B* **2014**, *196*, 429−433.
(22) Koh, A.; Kang, D.; Xue, Y.; Lee, S.; Pielak, R. M.; Kim, J.; Hwang, T.; Min, S.; Banks, A.; Bastien, P.; Manco, M. C.; Wang, L.; Ammann, K. R.; Jang, K.-I.; Won, P.; Han, S.; Ghaffari, R.; Paik, U.; Slepian, M. J.; Balooch, G.; Huang, Y.; Rogers, J. A. A soft, wearable microfluidic device for the capture, storage, and colorimetric sensing of sweat. *Sci. Transl. Med.* **2016**, *8*, 366ra165.
(23) Pellitero, M. A.; Guimerà, A.; Kitsara, M.; Villa, R.; Rubio, C.; Lakard, B.; Doche, M.-L.; Hihn, J.-Y.; Javier del Campo, F. Quantitative self-powered electrochromic biosensors. *Chem. Sci.* **2017**, *8*, 1995−2002.
(24) Zhang, H.; Yu, Y.; Zhang, L.; Dong, S. Fuel-free bio-photoelectrochemical cells based on a water/oxygen circulation system with a Ni:FeOOH/BiVO4Photoanode. *Angew. Chem., Int. Ed.* **2018**, *57*, 1547−1551.
(25) Narváez Villarrubia, C. W.; Rincón, R. A.; Radhakrishnan, V. K.; Davis, V.; Atanassov, P. Methylene green electrodeposited on SWNTs-based "bucky" papers for NADH and L-malate oxidation. *ACS Appl. Mater. Interfaces* **2011**, *3*, 2402−2409.
(26) Li, H.; Worley, K. E.; Calabrese Barton, S. Quantitative analysis of bioactive NAD+Regenerated by NADH electro-oxidation. *ACS Catal.* **2012**, *2*, 2572−2576.
(27) Zhang, X.; Guo, S.; Han, Y.; Li, J.; Wang, E. Beyond conventional patterns: New electrochemical lithography with high precision for patterned film materials and wearable sensors. *Anal. Chem.* **2017**, *89*, 2569−2574.
(28) Agarwal, R.; Sharma, M. K. A facile hybrid electrochemical-chemical approach to synthesize prussian blue from a single ferricyanide solution. *Electrochim. Acta* **2017**, *235*, 129−134.
(29) Yu, Y.; Han, Y.; Lou, B.; Zhang, L.; Han, L.; Dong, S. A miniature origami biofuel cell based on a consumed cathode. *Chem. Commun.* **2016**, *52*, 13499−13502.
(30) Vastarella, W.; Nicastri, R. Enzyme/semiconductor nano-clusters combined systems for novel amperometric biosensors. *Talanta* **2005**, *66*, 627−633.
(31) Gross, A. J.; Holzinger, M.; Cosnier, S. Buckypaper bioelectrodes: emerging materials for implantable and wearable biofuel cells. *Energy Environ. Sci.* **2018**, *11*, 1670−1687.
(32) Rincón, R. A.; Artyushkova, K.; Mojica, M.; Germain, M. N.; Minteer, S. D.; Atanassov, P. Structure and electrochemical properties of electrocatalysts for NADH oxidation. *Electroanalysis* **2010**, *22*, 799−806.
(33) Jarjes, Z. A.; Samian, M. R.; Ab Ghani, S. Conductive polymers: their preparations and catalyses on NADH oxidation at carbon cloth electrodes. *Arab. J. Chem.* **2015**, *8*, 726−731.
(34) Funabashi, H.; Takeuchi, S.; Tsujimura, S. Hierarchical meso/macro-porous carbon fabricated from dual MgO templates for direct electron transfer enzymatic electrodes. *Sci. Rep.* **2017**, *7*, 45147.
(35) Li, H.; Li, R.; Worden, R. M.; Calabrese Barton, S. Facilitation of high-rate NADH electrocatalysis using electrochemically activated carbon materials. *ACS Appl. Mater. Interfaces* **2014**, *6*, 6687−6696.
(36) Zhou, D.-m.; Fang, H.-Q.; Chen, H.-y.; Ju, H.-x.; Wang, Y. The electrochemical polymerization of methylene green and its electrocatalysis for the oxidation of NADH. *Anal. Chim. Acta* **1996**, *329*, 41−48.
(37) Osman, M. H.; Shah, A. A.; Walsh, F. C. Recent progress and continuing challenges in bio-fuel cells. Part I: enzymatic cells. *Biosens. Bioelectron.* **2011**, *26*, 3087−3102.
(38) Gauthier, E.; Hellstern, T.; Kevrekidis, I. G.; Benziger, J. Drop detachment and motion on fuel cell electrode materials. *ACS Appl. Mater. Interfaces* **2012**, *4*, 761−771.
(39) Philip, D Green synthesis of gold and silver nanoparticles using hibiscus rosa sinensis. *Phys. E* **2010**, *42*, 1417−1424.
(40) Guo, S.; Wang, L.; Wang, E. Templateless, surfactantless, simple electrochemical route to rapid synthesis of diameter-controlled 3D flowerlike gold microstructure with "clean" surface. *Chem. Commun.* **2007**, 3163−3165.
(41) Qiu, J.-D.; Peng, H.-Z.; Liang, R.-P.; Li, J.; Xia, X.-H. Synthesis, characterization, and immobilization of Prussian blue-modified Au nanoparticles: application to electrocatalytic reduction of H_2O_2. *Langmuir* **2007**, *23*, 2133−2137.
(42) Zhai, J.; Zhai, Y.; Dong, S. Direct dissolution of Au nanoparticles induced by potassium ferricyanide. *Colloids Surf., A* **2009**, *335*, 207−210.
(43) del Torno-de Román, L.; Alonso-Lomillo, M. A.; Domínguez-Renedo, O.; Merino-Sánchez, C.; Merino-Amayuelas, M. P.; Arcos-Martínez, M. J. Fabrication and characterization of disposable sensors and biosensors for detection of formaldehyde. *Talanta* **2011**, *86*, 324−328.
(44) Wang, X.; Cui, F.; Lin, J.; Ding, B.; Yu, J.; Al-Deyab, S. S. Functionalized nanoporous TiO2 fibers on quartz crystal micro-balance platform for formaldehyde sensor. *Sens. Actuators, B* **2012**, *171-172*, 658−665.
(45) Dong, S.; Dasgupta, P. K. Solubility of gaseous formaldehyde in liquid water and generation of trace standard gaseous formaldehyde. *Environ. Sci. Technol.* **1986**, *20*, 637−640.

DOI: 10.1021/acssensors.9b00917
ACS Sens. 2019, 4, 2631−2637